

# A New Active Snubber Circuit for PFC Converter

Burak Akin

Yildiz Technical University/Electrical Engineering Department, Istanbul, TURKEY  
Email: bakin@yildiz.edu.tr

**ABSTRACT**—In this paper, a new active snubber circuit is developed for PFC converter. This active snubber circuit provides zero voltage transition (ZVT) turn on and zero current transition (ZCT) turn off for the main switch without any extra current or voltage stresses. Auxiliary switch turns on and off with zero current switching (ZCS) without voltage stress. Although there is a current stress on the auxiliary switch, it is decreased by diverting it to the output side with coupling inductance. The proposed PFC converter controls output current and voltage in very wide line and load range. This PFC converter has simple structure, low cost and ease of control as well. In this study, a detailed steady state analysis of the new converter is presented, and the theoretical analysis is verified exactly by 100 kHz and 300 W prototype. This prototype has 98% total efficiency and 0.99 power factor with sinusoidal current shape.

**Index Terms**— Power factor correction (PFC), soft switching (SS), ZCS, ZCT, and ZVT.

## I. INTRODUCTION

In recent years, the power electronic systems and devices, which are used more frequently, create harmonic currents and pollute the electricity network. Harmonics have a negative effect on the operation of the receiver, who is feeding from the same network. Some sensitive equipments cannot work right. Nowadays, designers provide all the electronic devices to meet the harmonic content requirements.

AC-DC converters have drawbacks of poor power quality in terms of injected current harmonics, which cause voltage distortion and poor power factor at input ac mains and slow varying ripples at dc output load, low efficiency and large size of ac and dc filters [8]. These converters are required to operate with high switching frequencies due to demands for small converter size and high power density. High switching frequency operation, however, results in higher switching losses, increased electromagnetic interference (EMI), and reduced converter efficiency [13]. To overcome these drawbacks, low harmonic and high power factor converters are used with soft switching techniques. High switching frequency with soft switching provides high power density, less volumes and lowered ratings for the components, high reliability and efficiency [1-3], [7], [10], [12], [13], [16].

In principle, the switching power losses consist of the current and voltage overlap loss during the switching period, power diode's reverse recovery loss and discharge energy loss of the main switch parasitic capacitance. Soft switching with Pulse Width Modulation (PWM) control has four main groups as zero voltage switching (ZVS), zero current switching (ZCS), zero voltage transition (ZVT) and zero current switching (ZCT). ZVS and ZCS provides a soft switching, but ZVT and ZCT techniques are advanced, so switching power loss can be completely destroyed or is diverted to entry or exit [10].

In this study, to eliminate drawbacks of the PFC converters, the new active snubber circuit is proposed. The proposed circuit provides perfectly ZVT turn on and ZCT turn off together for the main switch, and ZCS turn on and turn off for the auxiliary switch without an important increase in the cost and complexity of the converter. There are no additional current or voltage stresses on the main switch. A part of the current of the auxiliary switch is diverted to the output with the coupling inductance, so better soft switching condition is provided for the auxiliary switch. Serially added  $D_2$  diode to the auxiliary switch path prevents extra current stress for the main switch. The aim of this proposed converter is to achieve high efficiency and high switching frequency PFC converter with sinusoidal current shape and unity power factor at universal input. The steady state operation of the new converter is analyzed in detail, and this theoretical analysis is verified exactly by a prototype of a 300 W and 100 kHz boost converter.

## II. OPERATION PRINCIPLES AND ANALYSIS

### Definitions and Assumptions

The circuit scheme of the new PFC converter is given in Fig. 1. In this circuit,  $V_i$  is input voltage source,  $V_o$  is output voltage,  $L_F$  is the main inductor,  $C_o$  is output capacitor,  $R$  is output load,  $S_1$  is the main switch,  $S_2$  is the auxiliary switch and  $D_F$  is the main diode. The main switch consists of a main switch  $S_1$  and its body diode  $D_{S1}$ .  $L_{R1}$  and  $L_{R2}$  are upper and lower snubber inductances,  $C_R$  is snubber capacitor, and  $D_1$ ,  $D_2$ ,  $D_3$  and  $D_4$  are the auxiliary diodes.  $L_m$  is the magnetization inductance;  $L_{il}$  and  $L_{ol}$  are the input and output leakage inductances of the transformer

respectively. Air gap and leakage inductance ratings are assumed sufficiently big enough.  $C_s$  is the equivalent parasitic capacitor of the main switch, so it is not an additional component to this converter.

For one switching cycle, the following assumptions are made in order to simplify the steady state analysis of the circuit shown in Fig. 1.

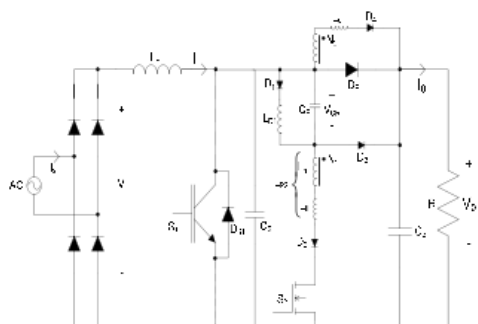


Figure 1. The circuit scheme of the proposed new PFC converter.

put voltage  $V_o$  and input current  $I_i$  are constant for one switching cycle, and all semiconductor devices and resonant circuits are ideal. Furthermore, the reverse recovery times of all diodes are not taken into account.

#### Operation Stages

Twelve stages occur over one switching cycle in the steady state operation of the proposed converter. The equivalent circuit schemes of the operation stages are given in Fig. 2 (a)-(l) respectively. The key waveforms concerning the operation modes are shown in Fig. 3. The detailed analysis of every mode of this converter is presented below.

##### Stage 1 [ $t_0 < t < t_1$ : Fig.2(a) ]

First of all,  $S_1$  and  $S_2$  switches are in the off state.  $I_i$  input current passes through the  $D_F$  main diode at this stage. At  $t=t_0$ ,  $i_{S1}=0$ ,  $i_{S2}=0$ ,  $i_{DF}=I_i$ ,  $i_{LR1}=0$ ,  $i_{LR2}=0$  and  $v_{CR}=0$  are valid. When the gate signal is applied to the  $S_2$ , a resonance starts between  $L_{R1}$ ,  $L_{R2}$  and  $C_R$ . Then,  $S_2$  current rises meanwhile  $D_F$  current falls.  $L_{R2}$  snubber inductance provides turn on switching with ZCS of  $S_2$ ,  $D_1$  and  $D_2$ .

In this interval, depending on transformer conversion ratio, input and output currents of transformer rise and  $D_F$  current falls. At  $t=t_1$ , the sum of the input and output currents of transformer reaches to  $I_i$  input current and then,  $D_F$  current falls to zero and  $D_F$  turns off with ZCS.

##### Stage 2 [ $t_1 < t < t_2$ : Fig.2(b) ]

The main switch  $S_1$  and the main diode  $D_F$  are in off state and  $S_2$  is in on state. At  $t=t_1$  a resonance starts between  $C_s$ - $L_{R1}$ - $L_{R2}$ - $C_R$ . The main switch's parasitic capacitor  $C_s$  discharges, at the same time the energy in  $L_{R2}$  is transferred to the output side by the coupling inductance. At  $t=t_2$ ,  $V_{CS}$  voltage becomes zero and  $D_{S1}$

turns on with ZVS, meanwhile  $D_4$  turns off and this interval ends.

##### Stage 3 [ $t_2 < t < t_4$ : Fig.2(c) ]

$D_{S1}$  is turned on at  $t_2$ . The resonant between  $L_{R1}$ - $L_{R2}$ - $C_R$  continues. After this stage  $L_{R2}$  inductance value is equal to the sum of  $L_{L1}$  and  $L_m$ .

In this stage,  $D_{S1}$  diode conducts the excess of  $L_{R2}$  current from the input current. The interval of this stage is time for the main switch  $S_1$  to turn on with zero voltage transition (ZVT). During this zero voltage transition time, gate signal must be applied to the main switch  $S_1$ . So  $S_1$  can be turned on with both ZVS and ZCS by ZVT. At  $t=t_3$ ,  $L_{R2}$  current drops to the input current, so  $D_{S1}$  turns off with ZCS and  $S_1$  turns on with ZVT. The main switch current starts to rise. At  $t=t_4$   $S_1$  current reaches to the input current level and  $L_{R2}$  current becomes zero. When the auxiliary switch current becomes zero, it is time to cut off the gate signal of  $S_2$ . So, the auxiliary switch  $S_2$  perfectly turns off with ZCS.

##### Stage 4 [ $t_4 < t < t_5$ : Fig.2(d) ]

This interval starts at  $t=t_4$  when  $S_2$  switch is turned off. While  $S_1$  conducts input current  $I_i$ , a resonance occurs through  $L_{R1}$ - $C_R$ - $D_1$ . The energy in  $L_{R1}$  is transferred to the  $C_R$  with this resonant. At  $t=t_5$ , this stage ends when  $L_{R1}$  current is equal to zero and  $C_R$  voltage reaches its maximum level.

##### Stage 5 [ $t_5 < t < t_6$ : Fig.2(e) ]

During this period, the main switch  $S_1$  conducts input current  $I_i$  and the snubber circuit is not active. The duration of this interval is a large part of the on state duration of the standard PWM boost converter and is determined by the PWM control to provide PFC.

##### Stage 6 [ $t_6 < t < t_8$ : Fig.2(f) ]

At  $t=t_6$ , when the control signal of the auxiliary switch  $S_2$  is applied, a new resonance starts between snubber inductance  $L_{R2}$  and snubber capacitor  $C_R$  through  $C_R$ - $L_{R2}$ - $S_2$ - $S_1$ .

The auxiliary switch  $S_2$  turned on with ZCS through  $L_{R2}$ . The auxiliary switch current rises and the main switch current falls due to the resonance. At  $t=t_7$ , when the  $S_2$  current reaches input current level, the main switch current becomes zero. After  $S_1$  current falls to zero  $D_{S1}$  is turned on with ZCS. There is zero current and zero voltage on the main switch  $S_1$ . So it is time to cut off the gate signal of  $S_1$  to provide ZCT. A new resonance occurs through the way of  $C_R$ - $L_{R2}$ - $S_2$ - $D_{S1}$ .  $D_{S1}$  conducts the excess of  $i_{LR2}$  from the input current. At  $t=t_8$ ,  $v_{CR}$  falls to zero and  $i_{LR2}$  current reaches its maximum levels and this interval ends.

##### Stage 7 [ $t_8 < t < t_9$ : Fig.2(g) ]

At  $t=t_8$ , while  $v_{CR}$  voltage starts to be positive,  $D_1$  diode is turned on. A resonance starts between  $L_{R2}$ ,  $L_{R1}$

and  $C_R$ .  $L_{R2}$  current falls again to  $I_i$  and  $D_{S1}$  current becomes zero. At  $t=t_9$ , the diode  $D_{S1}$  turns off with ZCS. The duration of the on time of the  $D_{S1}$  is equal to the ZCT time.

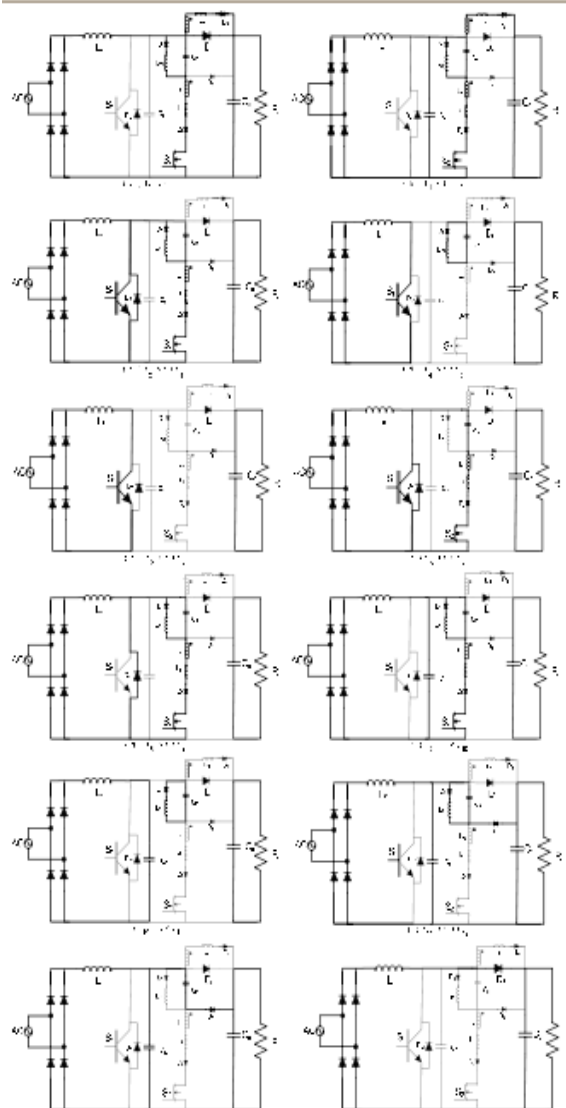


Figure 2. Equivalent circuit schemes of the operation modes

#### Stage 8 [ $t_9 < t < t_{10}$ : Fig.2(h) ]

At  $t=t_9$ , because  $i_{LR2}$  current falls to  $I_i$ , a resonance occurs between  $C_S$ - $L_{R1}$ - $L_{R2}$ - $C_R$  with this current.  $i_{LR2}$  current falls, and at  $t=t_{10}$ , when  $i_{LR2}$  current is equal to zero,  $S_2$  can be turned off. So the auxiliary switch  $S_2$  is turned off perfectly under ZCS.

#### Stage 9 [ $t_{10} < t < t_{11}$ : Fig.2(i) ]

There are two different closed circuits for this interval. For the first closed circuit,  $C_S$  capacitor is charged linearly with  $I_i$  and for the second closed circuit, a resonance occurs through  $L_{R1}$ - $C_R$ - $D_1$ . At  $t=t_{11}$  the sum of  $v_{CS}$  and  $v_{CR}$  voltages is equal to  $V_o$ , so  $D_3$  diode can be turned on.

#### Stage 10 [ $t_{11} < t < t_{12}$ : Fig.2(j) ]

A new resonance occurs through  $L_{R1}$ ,  $C_S$  and  $C_R$  with  $I_i$  input current. At  $t=t_{12}$ ,  $i_{LR1}$  current falls to zero, so this interval ends. The energy stored in  $L_{R1}$  inductance is transferred to the capacitors and load completely.

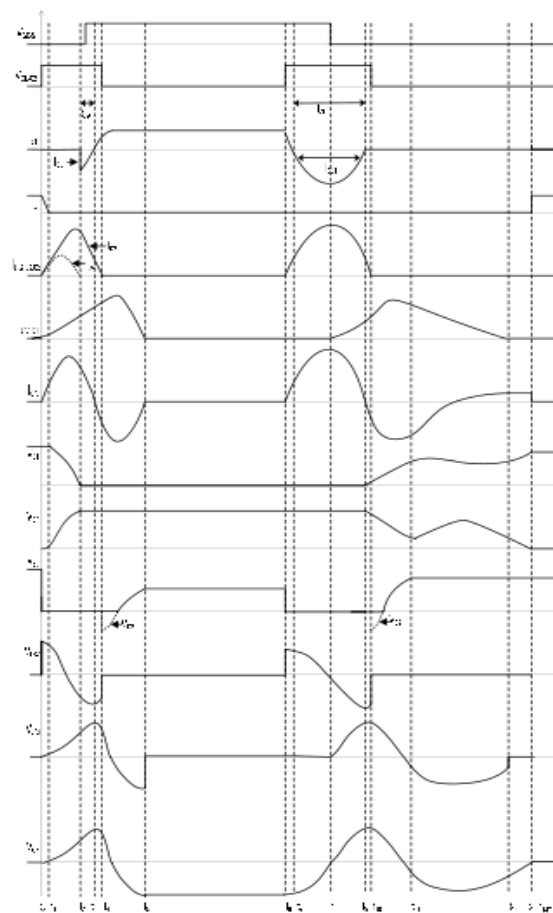


Figure 3. Key waveforms of the operation stages

#### Stage 11 [ $t_{12} < t < t_{13}$ : Fig.2(k) ]

$C_S$  is charged linearly with constant  $I_i$  current and  $C_R$  is discharged. At  $t=t_{13}$ , when  $C_S$  capacitor voltage reaches to  $V_o$ ,  $C_R$  capacitor voltage falls to zero and  $D_F$  diode is turned on with ZVS.

#### Stage 12 [ $t_{13} < t < t_{14}$ : Fig.2(l) ]

During this stage, the main diode  $D_F$  conducts input current  $I_i$  and the snubber circuit is not active. This time period is determined by the PWM control and large part of the off state of the converter. Finally, at  $t=t_{14}=t_0$ , one switching period is completed and then next switching period starts.

## EXPERIMENTAL RESULTS

A prototype of a 300 W and 100 kHz PFC converter is shown in Fig. 4 to verify the predicted analysis of the

proposed converter. The PFC converter is obtained by adding ZVT-ZCT-PWM active snubber circuit to the boost converter, which is fed by universal input AC line. The boost converter consists of the main inductance  $L_F$ , the main switch  $S_1$  with the antiparallel diode  $D_{S1}$  and the main diode  $D_F$ . The active snubber circuit consists of the auxiliary switch  $S_2$ , four auxiliary diodes  $D_1, D_2, D_3$ , and  $D_4$ , the snubber inductances  $L_{R1}$  and  $L_{R2}$  with the coupling inductance and the snubber capacitor  $C_R$ . For output receiver, resistive load is applied to the output of the converter.

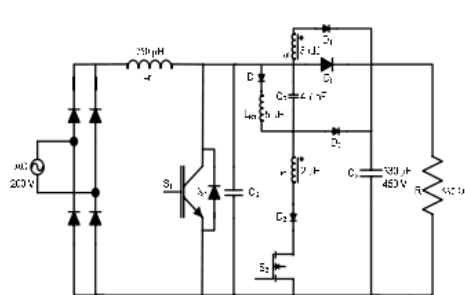


Figure 4. The prototype circuit scheme of the PFC converter.

The value of 200 V AC is applied to the input of the converter. Then, AC voltage is rectified to DC voltage for the boost converter. For the PFC converter, input bulk filter capacitor is not used after rectifier. This is because to control the line current to follow sinusoidal current for PFC. The  $L_F$  main inductance is calculated to process continues current mode (CCM) for the input line. The  $L_{R1}$  snubber inductance of the snubber circuit was chosen as 5  $\mu$ H, the  $L_{R2}$  snubber inductance as 2  $\mu$ H,  $L_{ol}$  the coupling inductance as 3  $\mu$ H and the  $C_R$  snubber capacitor as 4.7 nF. Input inductance  $L_F$  was chosen as 750  $\mu$ H to shape input current as sinusoidal and output capacitor  $C_o$  as 330  $\mu$ F to have constant output voltage.

In the Fig. 5 (a), the control signals of the main and the auxiliary switches are shown. The auxiliary switch operates twice in one switching cycle of the main switch and the main switch operates at 100 kHz. In Fig. 5 (b), it can be seen that  $S_1$  is operated under soft switching, for both turn on and turn off processes. Also, there are no overlap between voltage and current waveforms for the main switch  $S_1$ . During the turn on and turn off processes of the main switch  $S_1$ , its body diode is turned on. Therefore, ZVT turn on and ZCT turn off processes are perfectly realized for the main switch  $S_1$ . Furthermore, from the voltage waveform, there is no any additional voltage stress on the main switch. In the current waveform, there is a rising current to provide CCM for PFC converter.

In Fig. 5(c) the voltage and current waveforms of the auxiliary switch are shown. The auxiliary switch is operated in both ZVT and ZCT processes of the main switch  $S_1$  so, the auxiliary switch is operated at 200 kHz. Both ZVT and ZCT operations of the main

switch, the conduction time of the auxiliary switch is very short. The auxiliary switch is turned on and off under ZCS. Because the loss of the resonance circuit, the peak current of  $S_2$  in the ZCT interval is lower than the ZVT interval. And also the coupling inductance transfers the resonance energy to the output load for better efficiency. However, there are no additional voltage stresses on the semiconductors while the active snubber circuit operates under soft switching.

The main diode is turned on under ZVS and turned off under ZCS and ZVS. It can be seen in Fig. 5(d), there are no additional voltage and current stresses on the main diode. For the main and the auxiliary diodes, Silicon Carbide (SiC) diodes are used. SiC diodes have greater reverse recovery time with 10 ns.

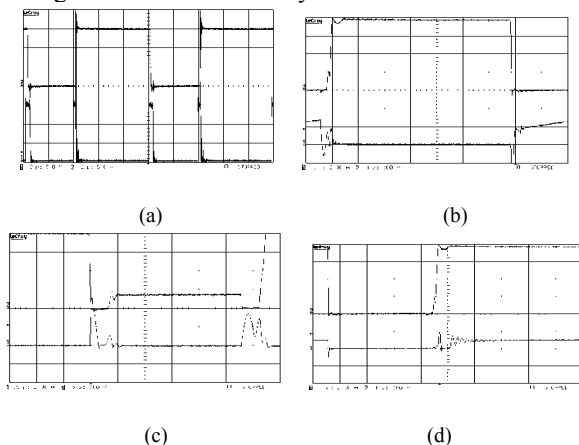


Figure 5. Some oscillograms of the PFC converter. a) Control signals of  $S_1$  and  $S_2$ . b) Voltage and current of  $S_1$ . c) Voltage and current of  $S_2$ . d) Voltage and current of  $D_F$ .

Input AC current and voltage waveforms can be seen in Fig. 6(a). The power factor of the proposed PFC converter is near unity with 0.99 value. Moreover, it is observed that the proposed PFC converter operates in CCM and keeps operating under soft switching conditions successfully for the whole line and load ranges. From Fig. 6(b), it is seen that the overall efficiency of the proposed PFC converter reaches a value of 98% at full output load.

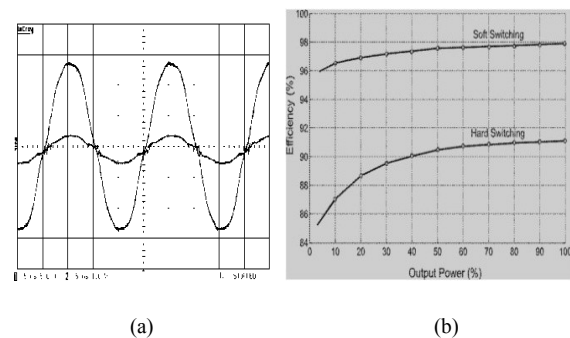


Figure 6. a) Voltage and current of input AC line b) Overall efficiency of the proposed converter

Because the converter power loss is dependent on circulating energy, it becomes lower as the load current falls in the proposed PFC converter.

### CONCLUSIONS

In this study, advanced and modern active snubber circuit is used for the new PFC converter. For this purpose, only one auxiliary switch and one resonant circuit is used. ZVT and ZCT techniques provide soft switching for the main switch and also for the other semiconductors. This new active snubber circuit is applied to the boost converter which is fed by rectified universal input AC line. As a result, the new PFC converter was carried out. This new PFC converter is realized with 200 V AC input mains, to provide 400 V DC output. The new PFC converter works with 100 kHz for 300 W output load. Oscilloscope and other measurement results are carried out briefly in this paper.

The main switch turns on with ZVT and turns off with ZCT, the auxiliary switch turns on and turns off with ZCS. Also, other semiconductors process with soft switching even at light load conditions. By the coupling inductance, current stress on the auxiliary switch is transferred to the output load to improve efficiency of the converter. The serially added diode to the auxiliary switch path prevents the incoming current stresses from the resonant circuit to the main switch. There are absolutely no current or voltage stresses on the main switch. Although there is no voltage stress on the auxiliary switch, the current stress is reduced by transferring this energy to the output load by the coupling inductance. Finally, at full load 98% efficiency is achieved. As a result, this new PFC converter has many desired features of the ZVT and ZCT converters and also it solves many drawbacks of the PFC converters. It was observed that the operation principles and the theoretical analysis of the new PFC converter were exactly verified by a 300 W and 100 kHz prototype. Additionally, at full output load, the new PFC converter reaches % 98 total efficiency and 0.99 power factor with sinusoidal current shape.

### REFERENCES

- [1] G. Hua, C. S. Leu, Y. Jiang, and F. C. Lee, "Novel Zero-Voltage-Transition PWM Converters," IEEE Transactions on Power Electronics, vol. 9, pp. 213-219, Mar. 1994.
- [2] G. Hua, E. X. Yang, Y. Jiang, and F. C. Lee, "Novel Zero-Current-Transition PWM Converters," IEEE Transactions on Power Electronics, vol. 9, pp. 601-606, Nov. 1994.
- [3] Lin R.L., Zhao Y., Lee F.C., "Improved Soft-Switching ZVT Converters with Active Snubber", Applied Power Electronics Conference and Exposition IEEE, vol. 2, pp. 1063 – 1069, Feb. 1998.
- [4] Singh K., Al. Haddad, and A. Chandra, "A review of active filters for power quality improvement," IEEE Transactions on Industrial Electronics, vol. 46, pp. 960–971, Oct. 1999.
- [5] M. Gotfryd, "Output Voltage and Power Limits in Boost Power Factor Corrector Operating in Discontinuous Inductor Current Mode", IEEE Transactions on Power Electronics, vol.15, pp. 51-57, Jan.2000.
- [6] Chongming Qiao, Keyue Ma Smedley, "A Topology Survey of Single-Stage Power Factor Corrector with a Boost Type Input-Current-Shaper", IEEE Transactions on Power Electronics, vol.16, pp. 360-368, May 2001.
- [7] H. Bodur and A. F. Bakan, "A New ZVT-PWM DC-DC Converter," IEEE Transactions on Power Electronics, vol. 17, pp. 40-47, Jan. 2002.
- [8] Singh B., Singh B.N., Chandra A., Al-Haddad K., Pandey A., Kothari D.P., "A Review of Single-Phase Improved Power Quality AC–DC Converters", IEEE Transactions on Industrial Electronics, vol. 50, no. 5, 962- 982, October 2003.
- [9] De Gusseme K., Van de Sype D.M., Van den Bossche A.P., Melkebeek J.A., "Input Current Distortion of CCM Boost PFC Converters Operated in DCM", Power Electronics Specialist Conference, PESC '03, 34th Annual, vol. 4, pp. 1685 – 1690, June 2003.
- [10] H. Bodur, and A.F. Bakan, "A New ZVT-ZCT-PWM DC-DC Converter," IEEE Transactions on Power Electronics, vol. 19, pp. 676-684, May. 2004.
- [11] R. Brown, M. Soldano, "PFC Converter Design with One Cycle Control IC" International Rectifier, pp. 8-12, June 2005.
- [12] A.F. Bakan, H. Bodur, and I. Aksoy, "A Novel ZVT-ZCT PWM DC-DC Converter", 11th European Conference on Power Electronics and Applications (EPE2005), Dresden, 1-8, Sept. 2005.
- [13] Wannian Huang, Moschopoulos G., "A New Family of Zero Voltage Transition PWM Converters With Dual Active Auxiliary Circuits" IEEE Transactions on Power Electronics, vol. 21, pp. 370-379, March 2006.
- [14] Akin B., "Technical And Physical Problems In Single Phase AC-DC Power Factor Correction Boost Converters", 3. International Conference on "Technical and Physical Problems in Power Engineering" (TPE-2006), Ankara 29-31 May 2006.
- [15] Akin B., "Application of a Remote Lab: Single Phase PFC circuit", Interactive Mobile & Computer Aided Learning (IMCL 2006), Amman, 19-21 April 2006.
- [16] P. Das, and G. Moschopoulos, "A Comparative Study of Zero-Current-Transition PWM Converters", IEEE Transactions on Industrial Electronics, vol.54, pp. 1319-1328, June 2007.